Model-based Non-stationary Unbalance Identification

Benjamin Siegl[1]*, Richard Markert[1]

ISROMAC 2016

International Symposium on Transport Phenomena and Dynamics of Rotating Machinery

Hawaii, Honolulu

April 10-15, 2016

Abstract

In this paper a method for unbalance identification in time-domain is presented. It is capable to identify the unbalance from a single run-up (or run-down) process without using test weights. The novelty compared to previous works is that there are no limitations concerning speed-dependency of the system matrices in the equation of motion. This gives rise to the identification of systems, for example with gyroscopic effects or journal bearings. The permissibility of the simplifications made for the method will be demonstrated at synthetically generated time-signals. The functionality and robustness of the identification method will be proven experimentally using measured data of a rotor with distinctive gyroscopic effects.

Based on the resulting speed-dependent modal model, a numerical simulation in modal space gives a solution in time-domain. The identification algorithm is based on minimizing the squared error sum of these time signals transformed into physical coordinates and the measured time signals. The modal parameters have to be calculated or guessed for initial values of the algorithm. The algorithm stops after reaching a defined accuracy. Hence, the unbalance and modal parameters including their approximated speed-dependency are identified.

Keywords

Balancing — Gyroscopics — Identification

[1] *Institute of Strucural Dynamics, TU Darmstadt, Germany*

***Corresponding author**: siegl@sdy.tu-darmstadt.de

INTRODUCTION

Balancing of rotors is an established procedure which is necessary to guarantee the service life and efficiency of rotating machines [1]. Unbalances occur, if the central rotation axis is out of alignment with a central main inertia axis. This results in rotating fictitious forces which cause — usually unwanted and disadvantageous — vibrations and bearing forces. For a smooth running of the machine, material is added or removed to such an extent, that the initial unbalance is compensated. For that, the experimental identification of this initial unbalance is necessary.

In rotor systems it is possible that the generally non-symmetric system matrices become speed dependent, e. g. due to journal bearing or gyroscopic effects. This causes speed dependent eigen-values, modal masses and eigen-vectors. Because of the non-symmetric system matrices the right-eigenvectors and left-eigenvectors are unequal.

In this paper the suitability of the model-based unbalance identification in time domain out of one non-stationary measurement is verified for rotor systems with speed-dependent non-symmetric system matrices. The general feasibility of model-based unbalance identification from non-stationary measurements has been proved in frequency domain by Markert [2]. For speed-constant and symmetric matrices the potential of non-stationary balancing methods has been verified by Seidler in time domain and frequency domain [3, 4]. An application of the time-domain method to turbochargers based on partially constant eigen-vectors has been investigated by Kreschel [5] theoretically.

1. MODEL

The dynamic behavior of most rotors can be described by the equation of motion in the form [6, 7]

$$\boldsymbol{M}\,\ddot{\boldsymbol{q}} + (\boldsymbol{B}+\boldsymbol{G})\,\dot{\boldsymbol{q}} + (\boldsymbol{K}+\boldsymbol{N})\,\boldsymbol{q} = \boldsymbol{f} \tag{1}$$

with the displacement vector $\boldsymbol{q}$ and the vector of external forces $\boldsymbol{f}$. In eq. (1) the damping matrix $\boldsymbol{B}(\dot{\varphi})$ and the stiffness matrix $\boldsymbol{K}(\dot{\varphi})$ are symmetric while the gyroscopic matrix $\boldsymbol{G}(\dot{\varphi})$ and the circulatory matrix $\boldsymbol{N}(\dot{\varphi})$ are skew-symmetric. All of those matrices can depend on the rotor speed $\dot{\varphi}$ generally, especially for rotors with journal bearings or — as in this paper — gyroscopics. The general equation of motion (1) is transformed into state-space according to

$$\boldsymbol{A}_1\,\dot{\boldsymbol{x}} + \boldsymbol{A}_0\,\boldsymbol{x} = \boldsymbol{u} \tag{2}$$

with the physical state-vector $\boldsymbol{x}^T = [\boldsymbol{q}^T, \dot{\boldsymbol{q}}^T]$, the excitation vector $\boldsymbol{u}^T = [\boldsymbol{f}^T, \boldsymbol{0}^T]$ and the system matrices

$$\boldsymbol{A}_1 = \begin{bmatrix} \boldsymbol{B}+\boldsymbol{G} & \boldsymbol{M} \\ \boldsymbol{M} & \boldsymbol{0} \end{bmatrix} \quad \text{and} \quad \boldsymbol{A}_0 = \begin{bmatrix} \boldsymbol{K}+\boldsymbol{N} & \boldsymbol{0} \\ \boldsymbol{0} & -\boldsymbol{M} \end{bmatrix}.$$

Both system matrices can be speed-dependent what implicates a time-dependency. Because of the transience $\dot{\varphi}(t)$ the state-space in physical coordinates $\boldsymbol{x}(t)$ can be transformed in a speed-dependent modal state-space with the state vector $\boldsymbol{\xi}(t)$ using the right-modal matrix $\boldsymbol{X}^R(\dot{\varphi})$ according

$$\boldsymbol{X}^R\,\boldsymbol{\xi} = \boldsymbol{x}. \tag{3}$$

The speed-dependent right-modal matrix in eq. (3) can be also written as time-dependent, $\boldsymbol{X}^R(t)$, because of eq. (10), or a different speed-time relation $\dot{\varphi}(t)$. To transform eq. (2) into modal space the time-derivative of the transformation (3) is necessary. The term $\dot{\boldsymbol{X}}^R\boldsymbol{\xi}$ containing the time derivative of the right-modal matrix, occurring due the product rule for differentiation, is neglectable compared to $\boldsymbol{X}^R\dot{\boldsymbol{\xi}}$, so

$$\frac{\partial \boldsymbol{X}^R}{\partial t} \approx \boldsymbol{0} \quad \Longrightarrow \quad \boldsymbol{X}^R\dot{\boldsymbol{\xi}} = \dot{\boldsymbol{x}} \quad \text{but} \quad \frac{\partial \boldsymbol{X}^R}{\partial \dot{\varphi}} \neq \boldsymbol{0} \tag{4}$$

is obtained. Because of the aforementioned non-symmetry of the system matrices, for modal decoupling the left-modal matrix $\boldsymbol{X}^L$ is necessary [8]. Thus, premultiplication of eq. (2) with $\boldsymbol{X}^L$ and subsituting according eq. (4) yields

$$\begin{aligned} \boldsymbol{X}^{LT}\boldsymbol{A}_1\boldsymbol{X}^R &= \operatorname{diag}\{\ldots, a_n, \ldots\} \quad \text{and} \\ \boldsymbol{X}^{LT}\boldsymbol{A}_0\boldsymbol{X}^R &= -\operatorname{diag}\{\ldots, \lambda_n a_n, \ldots\} \end{aligned} \tag{5}$$

because of orthogonality, see [9]. In the obtained modal state-space, $a_n(t)$ are the generalized modal masses and $\lambda_n(t)$ are the corresponding eigen-values. For the final representation the system matrix

$$\boldsymbol{A}_\xi(t) = \operatorname{diag}\{\lambda_n(t)\}$$

and the excitation matrix

$$\boldsymbol{B}_\upsilon(t) = \operatorname{diag}\{1/a_n(t)\}\boldsymbol{X}^{LT}\boldsymbol{U}$$

is defined in the time-varying state-space. Additionally, the second time-derivative of the reference signal of the rotation [10] can be used as excitation vector

$$\boldsymbol{\upsilon} = \begin{bmatrix} -\cos\varphi(t) \\ \sin\varphi(t) \end{bmatrix}^{\bullet\bullet}. \tag{6}$$

This system excitation is measurable easily and is only dependent on the rotation angle φ of the rotor. The constant Matrix $\boldsymbol{U}$ contains the whole unbalance information comprising amplitudes and phase angles. Finally, the general form for the rotor dynamics of rotors with multiple degrees of freedem has been found:

$$\dot{\boldsymbol{\xi}} = \boldsymbol{A}_\xi(\dot{\varphi})\,\boldsymbol{\xi} + \boldsymbol{B}_\upsilon(\dot{\varphi})\,\boldsymbol{\upsilon}. \tag{7}$$

Depending on the effects that should be taken into consideration, the matrices in eq. (1) have to be composed. The special case of a single-disk rotor with gyroscopics will be discussed later in section 3.

2. ALGORITHM

The algorithm for unbalance identification is shown in figure 1 and works in time domain: Certain measurable signals of the state-vector $\widetilde{q}_n(t)$, $\dot{\widetilde{q}}_n(t)$ from the rotor during a fast run-up or a fast run-down process are taken as input for the algorithm. As reference signals, the sine and the cosine of the shaft angle are measured inputs, too. Before starting the identification loop, initial guesses for the eigen-values λ_n (eigen-frequencies ω_n, modal damping D_n) and right- and left-eigenvectors ($\hat{x}_n^R$, $\hat{x}_n^L$) and their speed-dependency have to be indicated. The initial guesses for these modal parameters could be taken from experimental or numerical modal analyses (EMA, NuMA).

After that, time signals in modal coordinates $\boldsymbol{\xi}(t)$ in the approximated modal state-space are calculated by numerical integration of eq. (7). Those modal time series are transformed into physical coordinates by using eq. (3). With available measured signals of the physical coordinates $\widetilde{\boldsymbol{q}}_\mathrm{r}(t)$ and the corresponding simulation signals $\boldsymbol{q}_\mathrm{r}(t)$ the residual vector

$$\boldsymbol{R}(t_c) = \widetilde{\boldsymbol{q}}_\mathrm{r}(t_c) - \boldsymbol{q}_\mathrm{r}(t_c) \tag{8}$$

is calculated at $c = [1, C]$ time reference points t_c. For the identification, the mean square error is minimized. It is calculated with the 2-norm of the reasonably normalized and dimensioned residual vector at each time reference point from eq. (8) using a nonlinear optimization algorithm (in this case `lsqnonlin` from the "Optimization Toolbox" in Matlab) by repeated gradient-based fitting [11] of the modal parameters and the unbalances $\boldsymbol{U}$,

$$\min_{\boldsymbol{\theta}} \sum_{c=1}^{C} \left|\boldsymbol{R}(t_c)\right|^2 \quad \Longrightarrow \quad \boldsymbol{\theta}. \tag{9}$$

The vector with the optimal parameter set $\boldsymbol{\theta}$ containing the searched unbalances is identified.

A known problem for such a high-dimensional nonlinear optimization problem can be getting stuck in local minima due to an improper initial value set. To avoid this problem, genetic algorithms or monte-carlo simluations could be used. In this paper, a different path was taken: To reduce the dimension of the parameter set, a pre-identification is made using the same alorithm scheme as shown in figure 1 but with a much simpler, Linear-Time-Invariant (LTI), system. The initial values for this pre-identification are taken from an experimental or numerical modal analysis (EMA), as aforementioned. The identification results of the LTI pre-identification are taken as initial values for the originally intended identification of the Linear(ized)-Time-Variant (LTV) system.

To minimize measuring errors, such as runout, and to improve the signal-noise ratio, it may be helpful to choose only the parts of the time signal near to the resonance for calculating the residual. Because the amplitudes are comparatively high in this areas, this works like a weighting procedure in the optimization procedure.

The major advantage of the modeling in modal space is that modes which are unexpected to be excited can be discarded, such as backward modes or modes in a different frequency range. Thus, a reduced modal model should be used for identification only conatining modes in the (relevant) frequency range of the rotor speed running through.

3. TEST ON A ROTOR WITH GYROSCOPICS

As a test object for the algorithm, the single-disk rotor with gyroscopics is used. A scheme of such a rotor can be seen in figure 2. Its behavior is well-known and is described in textbooks, such as Gasch [12].

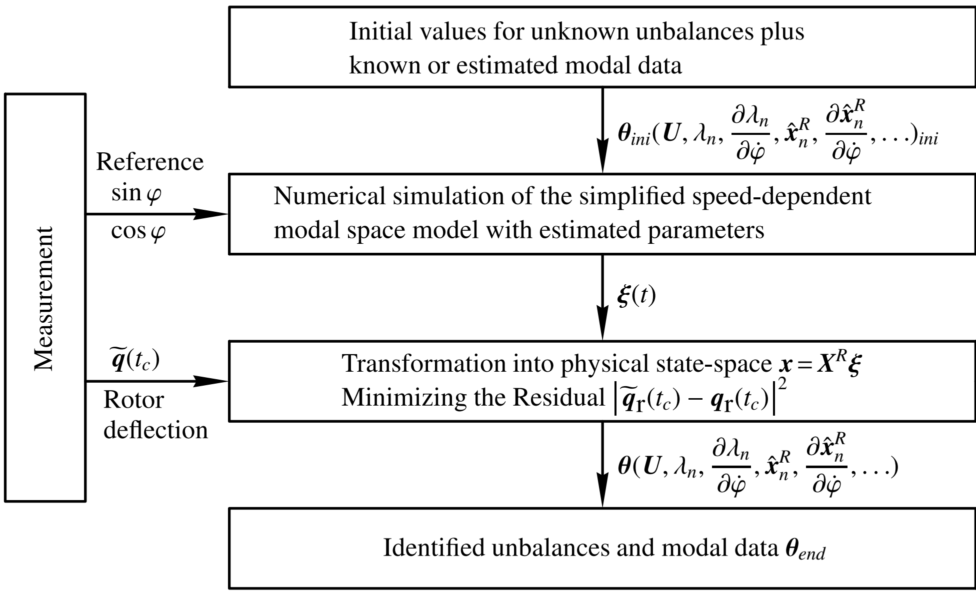

Figure 1. Algorithm for the unbalance identification in time domain

3.1 The Rotor

For the uniformly accelerated single-disk rotor with gyroscopics,

$$\dot{\varphi}(t) = \ddot{\varphi}\,t + \Omega_0 \quad \text{and} \quad \varphi(t) = \frac{1}{2}\ddot{\varphi}\,t^2 + \Omega_0\,t + \varphi_0 \qquad (10)$$

with the acceleration $\ddot{\varphi}$, the initial rotor speed Ω_0 and the initial shaft angle φ_0 the influence of the circulatory matrix $\boldsymbol{N}$ is neglectable, even for the comparatively high rotor acceleration of $\ddot{\varphi} = 3.2\ (2\pi/\mathrm{s})^2$ [13]. Thus, the matrices for the equation of motion (1) with the coordinate vector $\boldsymbol{q} = [\,w_W\ v_W\ \ -l_b\,\varphi_z\ l_b\,\varphi_y\,]^T$ are

$$\boldsymbol{M} = \begin{bmatrix} m & 0 & 0 & 0 \\ 0 & m & 0 & 0 \\ 0 & 0 & \Theta_a/l_b^2 & 0 \\ 0 & 0 & 0 & \Theta_a/l_b^2 \end{bmatrix},$$

$$\boldsymbol{B}+\boldsymbol{G} = \begin{bmatrix} b & 0 & 0 & 0 \\ 0 & b & 0 & 0 \\ 0 & 0 & b_\varphi & -\Theta_p/l_b^2\,\dot{\varphi} \\ 0 & 0 & \Theta_p/l_b^2\,\dot{\varphi} & b_\varphi \end{bmatrix} \quad \text{and}$$

$$\boldsymbol{K} = \begin{bmatrix} k_{11} & 0 & 0 & k_{12}/l_b \\ 0 & k_{11} & k_{12}/l_b & 0 \\ 0 & k_{12}/l_b & k_{22}/l_b^2 & 0 \\ k_{12}/l_b & 0 & 0 & k_{22}/l_b^2 \end{bmatrix}.$$

In the coordinate vector w_W is the vertical and v_W the horizontal lateral disk deflection. The twisting angle around the vertical z-axis multiplied with a reference-length l_b is described by $-l_b\,\varphi_z$, $l_b\,\varphi_y$ is analogical. The excitation vector because of unbalance due to a static eccentricity $|\varepsilon|$ with phase angle δ and a couple eccentricity $|\beta|$ with phase angle γ is

$$\boldsymbol{f} = \begin{bmatrix} |U_\varepsilon|\cos\delta & |U_\varepsilon|\sin\delta \\ |U_\varepsilon|\sin\delta & -|U_\varepsilon|\cos\delta \\ -|U_\beta|\cos\gamma & -|U_\beta|\sin\gamma \\ |U_\beta|\sin\gamma & -|U_\beta|\cos\gamma \end{bmatrix} \begin{bmatrix} -\cos\varphi \\ \sin\varphi \end{bmatrix}^{\bullet\bullet}.$$

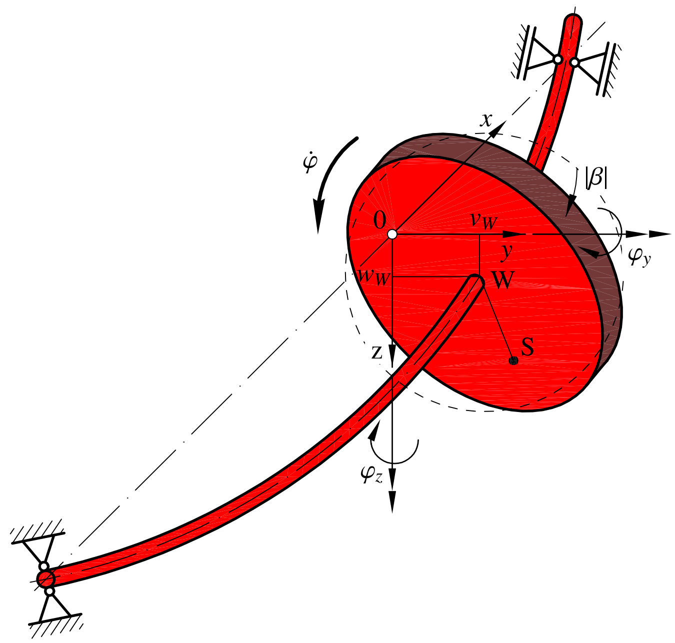

Figure 2. Scheme of the rotor model

It contains the static unbalance $U_\varepsilon = m\ |\varepsilon|\ e^{i\,\delta}$ and the couple unbalance $U_\beta = (\Theta_a - \Theta_p)\ |\beta|\ e^{i\,\gamma}/l_b$. The influence of the rotor weight can be suppressed by using a high-pass filter (AC coupling) in the measuring chain so it is not taken into account in the model.

Due to the gyroscopics, the modes of such a rotor are speed-dependent. For the model these dependencies are approximated by linear functions, as displayed in figure 3 and figure 4.

To prove the simplifications

a) the linear approximation of the modal data,

b) the negligience of the time-derivative $\dot{\boldsymbol{X}}^R$ and

c) omitting the backward and non-resonating modes

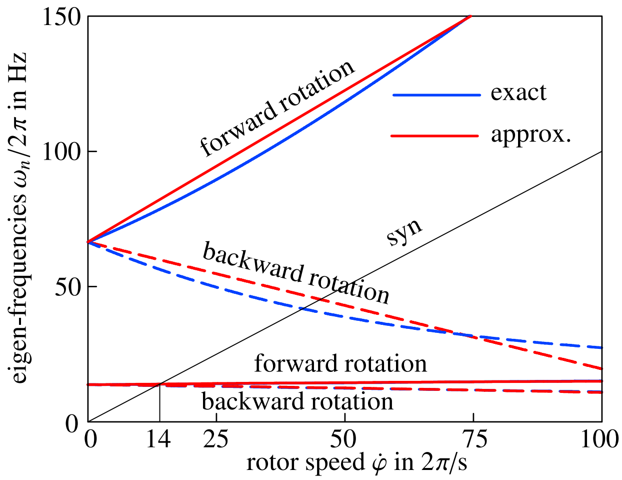

Figure 3. Speed-dependent eigen-frequencies

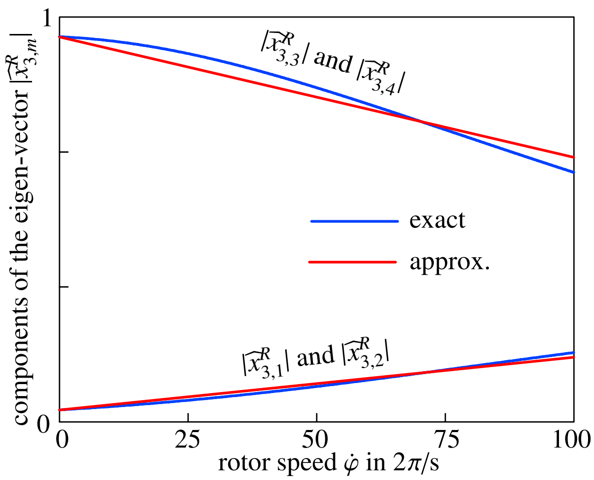

Figure 4. Speed-dependent entries of the 3rd eigen-vector

being permitted, a pre-simulation with the known eccentricities $\varepsilon = 3\cdot 10^{-4}$ m and $\beta = 0$ is made. It is calculated as a fast run-up from standstill to $\dot{\varphi}_{\max} = 100\cdot 2\pi/\mathrm{s}$ with known modal data corresponding to figures 3 and 4.

Figure 5 compares the exact time-integration of the single-disk rotor from figure 2 and the integration of the simplified model. The differences are invisibly small (especially in resonance at ~1 s). So it can be stated, that the simplifications (linear approximation of the modal data, neglecting modes which do not get into resonance and ignoring the time-derivatives of the right-eigenvectors) are permitted in the run-through frequency range.

The parameters of the rotor used for the artificially generated measurements, pre-simulations and approximately the test rig are stated in table 1. They are based on a work of Wegener [14] because this rotor is available for experimental investigations.

3.2 Results

To prove the algorithm from figure 1 working in reality and to test its robustness against measuring errors, deflections of the disk $\widetilde{\boldsymbol{q}}$ are taken at a rotor test rig showing distinctive gyroscopic effects. A photograph of the used test rig with the rotor data from table 1 is shown in figure 6.

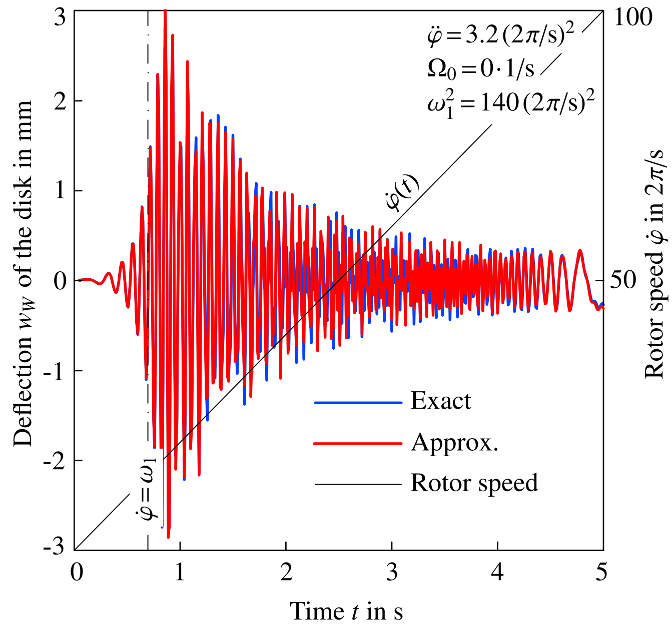

Figure 5. Deflection $w_W(t)$ during a fast run-up with and without approximations

Table 1. Rotor data

m	Θ_p	Θ_a	k_{11}	k_{12}	k_{22}
2.55 kg	$1.1\cdot 10^{-4}$ kg m^2	$6.6\cdot 10^{-3}$ kg m^2	$2.9\cdot 10^{4}$ N/m	$3.3\cdot 10^{3}$ N/rad	$1.1\cdot 10^{3}$ N m/rad

The unbalance mounted on the balanced test rotor was

$$U_\varepsilon = 3.2\cdot 10^{-4}\,\mathrm{kg\,m} \angle 30^\circ \quad \text{and} \quad U_\beta = 0\,\mathrm{kg\,m} \angle 0^\circ$$

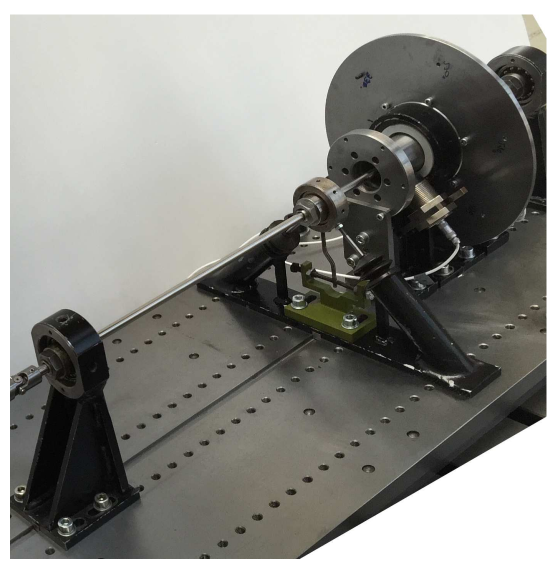

Figure 6. Photograph of the test rig

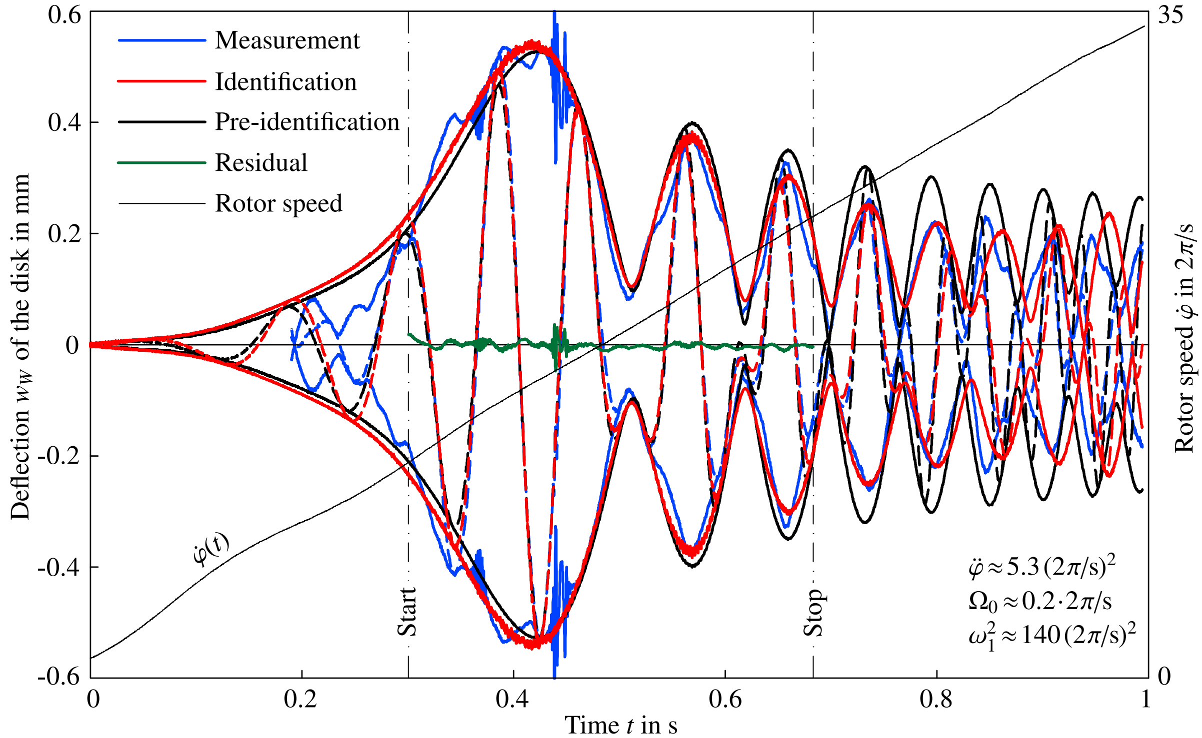

Figure 7. Deflection $w_W(t)$ in the last steps of the identification

which has to be identified. As starting values in the parameter vector $\boldsymbol{\theta}$ for both complex unbalances $U_\varepsilon = 0$ and $U_\beta = 0$ were used. The starting values for the eigen-values and eigen-vectors have been taken from a Theoretical Modal Analysis (TMA) of the non-rotating system with the data from table 1. To get a better guess for the initial values of the algorithm (figure 1) taking speed-dependent modal data into account, the pre-identification of the LTI system without gyroscopic effects (usually called Laval or Jeffcott rotor) was made.

For the residual $\boldsymbol{R}$ from eq. (8) the measured and simulated data for the lateral deflections in z- and y-direction, w_W and v_W, were utilized. In general, also the tilting angles φ_z and φ_y could be used but in this case it was not necessary, the identification result (figure 7) was sufficient.

Figure 7 shows the deflections in z-direction (dashed) and the corresponding envelopes (solid): The results of the measurement are drawn in blue, the results of the pre-identification using an LTI system in black. The results of the actual algorithm using the LTV system described in eqs. (1) to (7) are drawn in red. The thin dash-dotted black lines mark the time range with high amplitudes in which the resonance is passed and which is used for the identification. The thin solid black line is the measured rotor speed during the run-up, which is almost linear in this case (but not required by the algorithm).

In the envelope curve of the measurement at about 0.45 s a modulation with ~4 kHz is visible. This modulation comes from the perpendicular measuring channel in y-direction. The sensor (eddy-current displacement sensor) has a modulation frequency of ~4 kHz. Due to the small diameter of the measuring surface on the rotor side (50 mm) both sensors can influence each other at high amplitudes.

The solver for the nonlinear optimization problem from eq. (8) quits as soon as the difference

$$\sum_{c=1}^{C} \left|\boldsymbol{R}(t_c)\right|_j^2 - \sum_{c=1}^{C} \left|\boldsymbol{R}(t_c)\right|_{j-1}^2 \leq 10^{-6}\,\mathrm{mm} \tag{11}$$

of the quadratic residual norm between two iteration steps is sufficiently small. The remaining residual after the last step is pictured in figure 7 in green. Apparently, the range of the green curve does not cover the whole time range. This is because the algorithm only takes the area around the resonance to minimize measuring errors such as runout. A tightening of the abort criterion from eq. (11) does not lead to smaller residuals. The conclusion is that with the used model and the used initial values the best possible model fit is achieved.

In table 2 the resulting unbalances as well as the initial values for the LTI-identification and the LTV-identification and mounted unbalances at the test rig are listed. Because of the undefined phase angle, the initial values $U_\varepsilon = U_\beta = 0$ are the most inappropriate initial values possible. Nevertheless the balancing results are satisfying.

The computation time for this identification process was about 170 s on an Intel Core i7 with 3.4 GHz.

4. CONCLUSION AND OUTLOOK

In this paper the functionality of a time-domain algorithm for model-based unbalance identification was demonstrated

Table 2. Results of the unbalance identification

	U_ε	U_β
Aimed	$3.2\cdot10^{-4}\,\mathrm{kgm}\angle 30°$	$\sim 0\,\mathrm{kgm}\angle 0°$
Ini. values Pre-ident.	$0\,\mathrm{kgm}\angle 0°$	$0\,\mathrm{kgm}\angle 0°$
Ini. values Ident.	$4.2\cdot10^{-4}\,\mathrm{kgm}\angle 31.2°$	$\sim 0\,\mathrm{kgm}\angle 0°$
Results	$3.3\cdot10^{-4}\,\mathrm{kgm}\angle 31.3°$	$\sim 0\,\mathrm{kgm}\angle 0°$

in a practical application. The robustness of the simulation results against the linear approximation of the modal data, the neglegience of the time-derivative of the right-modal matrix and omitting the backward and non-resonating forward modes is the basis for the presented method. The advantage of the presented method is that is does not need test weights and uses a single run-up for unbalance (and system) identification.

The used single-disk rotor with gyroscopic effects was an academic example. The relative identification error was 3.1 % in amplitude and 1.3° in phase. This error is in the area of accuracy of the residual unbalance after balancing the test rotor with the standard method of influence coefficients.

The mechanism to get speed-dependent system matrices in this paper was gyroscopics. Compared to journal bearings the speed-dependency is weak. To prove the functionality also for rotors in journal bearings and the robustness against environmental impacts of the method at real machines in the next step it will be tested at an automotive turbocharger from serial production. The method itself should work as presented but the initial values for the modal data are more uncertain because it is impossible to determine reasonable modal data of a rotor in journal bearings at zero speed.

The limit of the presented method could be in nonlinear systems which can not be linearized, e. g. vertical rotors in cylindrical journal bearings because the linearized stiffness approaches zero. Simple extensions of the rotor model with linear or linearizable phenomena, such as multiple disks or more than two bearings, should not affect the functioning of the algorithm because it works in modal space and those phenomena would just cause additional modal coordinates.

REFERENCES

[1] Walter Kellenberger. *Elastisches Wuchten*. Springer-Verlag, 1987.

[2] Richard Markert. System- und Unwuchtidentifikation von elastischen Rotoren aus Anfahrmessungen. *VDI-Berichte*, 536:121–139, 1984.

[3] Malte Seidler. *Instationäres Auswuchten elastischer Rotoren*. Number 314 in Series 11: Schwingungstechnik. VDI Verlag, Düsseldorf, Dissertation, 2002.

[4] Malte Seidler and Richard Markert. Non-stationary Balancing of Flexible Rotors. *Zeitschrift für angewandte Mathematik und Mechanik (ZAMM)*, 81, Suppl. 2:429–430, 2001.

[5] Martin Kreschel. *Instationäres Verhalten von Abgasturboladern*. Number Nr. 731 in Reihe 12: Verkehrstechnik, Fahrzeugtechnik. VDI Verlag, Düsseldorf, Dissertation, 2010.

[6] Giancarlo Genta. *Dynamics of Rotating Systems*. Mechanical Engineering Series. Springer US, New York, NY, 2005.

[7] Richard Markert. *Strukturdynamik*. Shaker, Aachen, 1. auflage edition, September 2013.

[8] Rainer Nordmann. Modal parameter identification and sensitivity analysis in rotating machinery. In *IFToMM: Rotordynamic Problems in Power Plants*, Rome, Italy, 1982.

[9] Robert Gasch. *Strukturdynamik: Diskrete Systeme und Kontinua*. Springer, Berlin, auflage: 2. aufl. 2012 edition, 2012.

[10] Richard Markert. Modal Balancing of flexible rotors with data acquisition from non-stationary run-up or run-down. In *Proceedings of the VI. International Modal Analysis Conference*, pages 210–216, Orlando, Florida, 1988.

[11] Thomas F. Coleman and Y. Li. An Interior, Trust Region Approach for Nonlinear Minimization Subject to Bounds. *SIAM Journal on Optimization*, 6:418–445, 1996.

[12] Robert Gasch, Rainer Nordmann, and Herbert Pfützner. *Rotordynamik*. Springer, Berlin, 2. edition, 2006.

[13] Matthias Lauzi. Theoretische Untersuchungen an Rotoren mit Kreiselwirkung. Seminararbeit, TU Darmstadt, Darmstadt, 2012.

[14] Georg Wegener. Untersuchungen zum Kreiseleinfluß auf den stationären und instationären Betrieb von elastischen Rotoren. Diplomarbeit, TU Darmstadt, Darmstadt, 1993.